Temperature dependence of the energy transfer of exciton states in bilayer structures of CdSe/ZnS quantum dots

DaeGwi Kim,* Kanako Okazaki, and Masaaki Nakayama
Department of Applied Physics, Osaka City University, Sugimoto, Osaka 558-8585, Japan
(Received 15 March 2009; revised manuscript received 23 June 2009; published 28 July 2009)

We have investigated the temperature dependence of an energy transfer (ET) between CdSe/ZnS quantum dots (QDs) measuring photoluminescence dynamics in a bilayer structure consisting of differently sized QDs. In the bilayer structure, an effective direct ET from donor QDs to acceptor QDs is realized. The temperature dependence of the observed ET rate can be classified into two categories. Under the condition that the thermal energy (k_BT) is comparable to the splitting energy between the bright- and dark-exciton states and above, the observed ET rate is dominated by the thermal population behavior of the bright-exciton state: the ET rate increases with an increase in temperature. On the other hand, in the lower temperature region, the observed ET rate is almost constant, which may be due to a breakdown of the thermal equilibrium between the lower-lying dark-exciton state and the bright-exciton state.

DOI: 10.1103/PhysRevB.80.045322 PACS number(s): 78.67.Hc, 78.55.Et, 78.67.Pt

I. INTRODUCTION

In the past decades, semiconductor quantum dots (QDs) have been intensively investigated to understand the size dependence of their physical/chemical properties, where randomly dispersed QDs have been the major target in most of the studies so far.[1–4] Recently, the dynamical process of a resonant energy transfer (ET) between CdSe QDs was reported.[5,6] This pioneering work stimulated studies on QD-based ET processes employing QDs as energy donors in a QD-bioconjugate system[7] and a QD-organic dye system[8,9] as well as the ET process between QDs.[10,11]

One of the most characteristic PL properties of QDs is the observation of an optically passive state, the so-called dark-exciton state.[12–15] The origin of the dark-exciton state is basically attributed to a spin-triplet state that is forbidden for optical transitions by the spin-selection rule. Thus, it is considered that the Förster ET, which is due to a dipole-dipole interaction, from the dark-exciton state does not occur. The dark-exciton state mainly contributes to PL processes at low temperatures and the population in the upper-lying bright-exciton state is increased with an increase in temperature by the thermal excitation.[16,17] So far, most of studies on the ET process between QDs have been conducted at room temperature and little attention has been paid to the temperature dependence of ET dynamics. Thus, whether the Förster ET between QDs is suppressed at low temperatures is open question. In Ref. 11, Wuister *et al.* reported the temperature-dependent ET in CdTe QD solids. The decrease in ET rate with a decrease in temperature was explained qualitatively by the decreased dipole strength of the excitonic emission of QDs due to the presence of a singlet and lower-lying triplet state.[11] Since the splitting energy between the bright and dark-exciton states in CdSe QDs is much larger than that in CdTe QDs,[13] it is expected that CdSe QDs are suitable for the study on the temperature dependence of ET dynamics.

As shown in the inset in Fig. 1, we fabricated bilayer structures consisting of differently sized CdSe/ZnS QDs. In this structure, the efficient "*vertical*" ET from smaller QDs to larger QDs is realized like a donor-acceptor system.[6,18] We discuss the temperature dependence of ET dynamics between CdSe/ZnS QDs measuring photoluminescence dynamics in the bilayer structure.

II. EXPERIMENTS

CdSe/ZnS core/shell QDs with two different sizes (~4 and ~6 nm in diameter) were purchased from Evident Technologies (Evidots™, Troy, New York). The substrates of quartz were cleaned by immersion in fresh piranha solution [1/3 (v/v) mixture of 30% H_2O_2 and 98% H_2SO_4] for 20 min. Then the substrates were rinsed with water and then used immediately after cleaning. In the beginning of the sample preparation, self-assembled monolayers (SAMs) of (3-mercaptopropyl)trimethoxysilane (MPTMS) molecules were deposited to anchor QDs. The bilayer structures consisting of differently sized QDs were composed of three main blocks; the monolayer of larger QDs, which acts as energy acceptor QDs (A-QDs), followed by SAMs of dithiol linkers (1,2-ethanedithiol), and the monolayer of smaller QDs as energy donor QDs (D-QDs). The monolayer structure of the D-QDs was deposited on the SAM of MPTMS molecules. The ET rate in the bilayer structures was estimated from the comparison of PL-decay profiles of the D-QDs in the bilayer and monolayer structures.

For PL measurements, the 325-nm line of a He-Cd laser was used as the excitation-light source and the emitted PL was analyzed with a single monochromator with a spectral resolution of 0.5 nm. For measurements of PL-decay profiles, a laser diode (405 nm, Hamamatsu PLP10–040) with a pulse duration of 100 ps and a repetition of 500 kHz was used as the excitation light. The pump fluence was 50 nJ/cm^2. The PL-decay profiles were obtained by a time-correlated single-photon counting method. The sample temperature was controlled using a closed-cycle helium-gas cryostat.

III. RESULTS AND DISCUSSION

Figure 1(a) shows absorption and PL spectra at room temperature (RT) of D-QDs and A-QDs dispersed in toluene

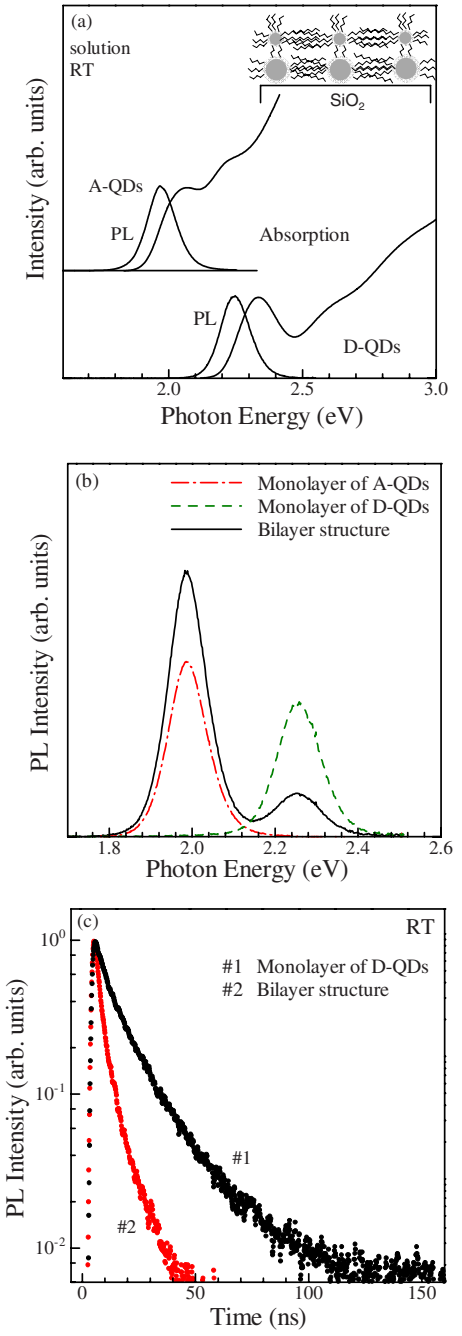

FIG. 1. (Color online) (a) Absorption and PL spectra of the D-QDs and A-QDs dispersed in toluene solution. Inset: schematic diagram of the bilayer structure consisting of differently sized CdSe/ZnS QDs. (b) PL spectra of the monolayer structures of the D-QDs and A-QDs (broken curves) and that of the bilayer structure (solid curve) at RT. (c) PL-decay profiles of the D-QDs in the monolayer and in the bilayer structure. The detection energy was 2.25 eV.

solution. In the PL spectrum, the band-edge PL band is dominant and a defect-related PL band is not observed at all. These results indicate the high crystallinity of CdSe/ZnS QDs. It is noted that the spectral overlap between the band-edge PL of the D-QDs and the absorption of the A-QDs is fully realized, which assures the effective ET from the D-QDs to the A-QDs in the bilayer structure. Figure 1(b) shows PL spectra of the monolayer structures of the D-QDs and A-QDs (broken curves) and that of the bilayer structure (solid curve) at RT. As compared to the PL properties of the monolayer structures, the PL quenching of the D-QDs, and the PL enhancement of the A-QDs are observed in the bilayer structure, which can be attributed to the ET from the D-QDs to the A-QDs. To investigate the ET rates, we measured PL-decay profiles. Figure 1(c) shows the PL-decay profiles of the D-QDs in the monolayer and in the bilayer structure. The detection energy was 2.25 eV. It is noted that the decay profiles of the D-QDs do not depend on the detection energy, indicating suppression of the in-plane ET process. The decay profile in the bilayer structure is faster than that in the monolayer of the D-QDs, which suggests that the shortened decay is due to the ET from the D-QDs to the A-QDs in the bilayer structure.

The decay profiles consist of multiple-exponential components as observed previously.[16,17] The analysis of multiple-exponential-decay profiles in colloidal QDs is still controversial. In order to discuss the PL-decay profiles quantitatively, we analyzed them by a stretched exponential function: $A\exp[-(t/\tau)^{\beta}]$. In general, $\beta<1$ represents the statistical distribution of exponential components with different decay times. In order to compare decay profiles in the monolayer and bilayer structures, we estimated an average decay time of $\langle\tau\rangle$ as in previous reports.[17,19] The energy-transfer rate (k_{ET}) in the bilayer structure can be estimated to be 0.05 ns^{-1} from the following expression: $k_{ET}=(1/\langle\tau_{bilayer}\rangle-1/\langle\tau_{monolayer}\rangle)$, where $\langle\tau_{monolayer}\rangle$ and $\langle\tau_{bilayer}\rangle$ are the average decay time of the D-QDs in the monolayer and bilayer structures, respectively.

Next, we discuss the temperature dependence of the ET process that is our motivation in the present work. Figure 2 shows the temperature dependence of PL spectra of the monolayer structures of the D- and A-QDs and the bilayer structure. From a comparison of PL spectra of the bilayer structure with those of the monolayer structures, the PL quenching of the D-QDs and the PL enhancement of the A-QDs in the bilayer structure are observed. These results obviously indicate the occurrence of the ET from the D-QDs in the bilayer structure at any temperature. So far, most of studies on the ET between QDs have been limited to discussion about the dynamics at room temperature. Kagan *et al.* reported that the ET rate increases at lower temperatures from a comparison of PL spectra at RT and 10 K in close-packed CdSe QD solids.[5] However, the PL efficiency at RT and 10 K was greatly different: 1.9% at RT and 24% at 10 K. Thus, nonradiative recombination processes considerably affect PL properties at RT, which is presumably due to the use of CdSe core QDs. In the present work, we used CdSe/ZnS core/shell QDs because it is well known that the growth in ZnS shell much improves their PL properties.

The inset in Fig. 2(a) shows the temperature dependence of the integrated PL intensity in the monolayer of the D-QDs. We note that the PL intensity at room temperature was almost 60% of that at 10 K, which means that the thermal-quenching effect is very small. The above results demonstrate that the nonradiative process is remarkably suppressed in CdSe/ZnS QDs, which is a merit of the use the core/shell QDs. To avoid the influence of the nonradiative recombina-

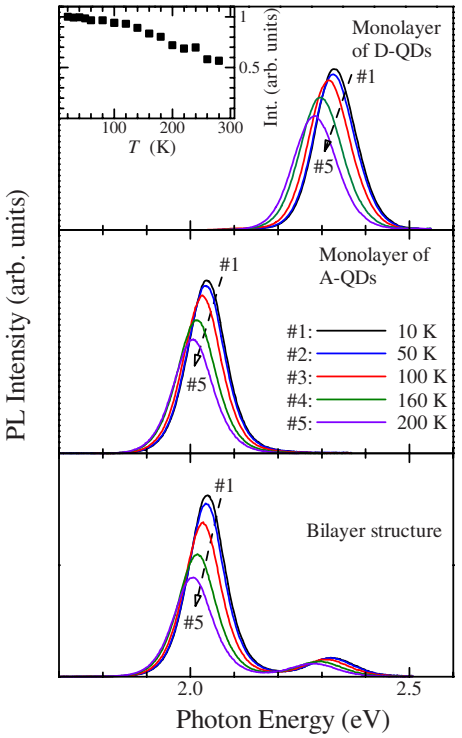

FIG. 2. (Color online) Temperature dependence of PL spectra of the monolayer structures of the D- and A-QDs and the bilayer structure. Inset: temperature dependence of the integrated PL intensity in the monolayer of the D-QDs.

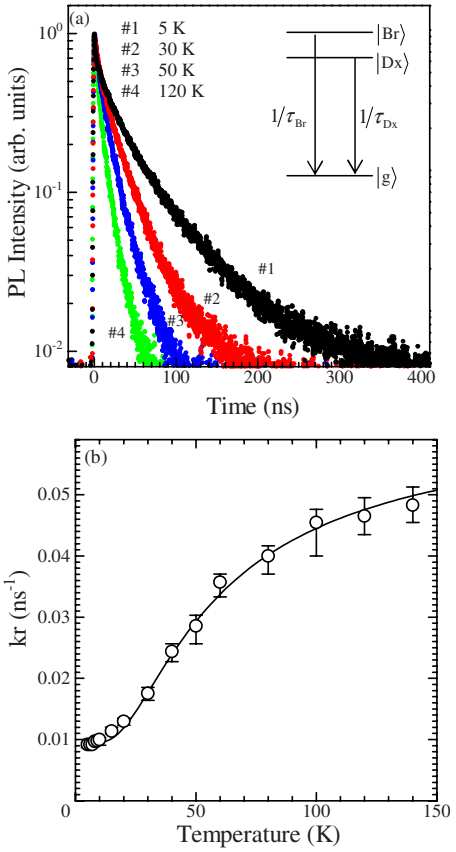

FIG. 3. (Color online) (a) Temperature dependence of PL-decay profiles of the monolayer structure of the D-QDs. Inset: the energy scheme of a three-state model consisting of a ground state and two excited states of $|\mathrm{Br}\rangle$ and $|\mathrm{Dx}\rangle$ (Ref. 16). (b) Temperature dependence of the PL-decay rate up to 140 K. The solid curve represents the calculated result using Eq. (3) with $\tau_{\mathrm{Br}}=8.4$ ns, $\tau_{\mathrm{Dx}}=110$ ns, and $\Delta E=6$ meV.

tion process as much as possible, we measured the PL-decay profiles in the temperature region up to 140 K because the PL intensity in this temperature region has 90% or more of that at 10 K.

Figure 3(a) shows the temperature dependence of PL-decay profiles of the monolayer structure of the D-QDs. The PL-decay profiles become faster with an increase in temperature as in previous reports.[16,17] The temperature dependence of PL dynamics in CdSe and/or CdSe/ZnS QDs can be understood by a three-state model (TSM) consisting of a ground state and two excited states: a lower-lying dark-exciton state and a higher-lying bright-exciton state.[16,17] On the basis of this model, we can expect that the population in the upper state with a fast decay component is increased with an increase in temperature by the thermal excitation from the lower state with a slow-decay component, leading to shortening the decay profiles. The observed decay profiles consist of multiple-exponential components as shown in Fig. 3(a). As described above, the average decay times were determined from the stretched exponential fitting in order to discuss the temperature dependence of the decay rate. Figure 3(b) shows the temperature dependence of the average PL-decay rate up to 140 K. In this temperature region, the decay rate can be regarded as "*radiative*" decay rate since the thermal quenching of the PL intensity is negligible.

The energy scheme of the TSM is shown in the inset of Fig. 3(a): a ground state $|\mathrm{g}\rangle$ and two excited states of the dark-exciton state $|\mathrm{Dx}\rangle$ and bright-exciton state $|\mathrm{Br}\rangle$. Here, $|\mathrm{Dx}\rangle$ lies below $|\mathrm{Br}\rangle$ by an energy spacing of ΔE. The rate equation for the number of the excitons in the TSM is given as

$$\frac{dn_{\mathrm{Br}}}{dt} = -\frac{1}{\tau_{\mathrm{Br}}}n_{\mathrm{Br}} - \frac{1}{\tau_{\mathrm{relax}}}n_{\mathrm{Br}} + \frac{1}{\tau_{\mathrm{relax}}}e^{-\Delta E/k_{\mathrm{B}}T}n_{\mathrm{Dx}}, \quad (1)$$

$$\frac{dn_{\mathrm{Dx}}}{dt} = -\frac{1}{\tau_{\mathrm{Dx}}}n_{\mathrm{Dx}} - \frac{1}{\tau_{\mathrm{relax}}}e^{-\Delta E/k_{\mathrm{B}}T}n_{\mathrm{Dx}} + \frac{1}{\tau_{\mathrm{relax}}}n_{\mathrm{Br}}, \quad (2)$$

where n_{Br} (n_{Dx}) and $1/\tau_{\mathrm{Br}}$ ($1/\tau_{\mathrm{Dx}}$) denote the exciton number and the radiative-decay rate of $|\mathrm{Br}\rangle$ ($|\mathrm{Dx}\rangle$), respectively. $1/\tau_{\mathrm{relax}}$ is the relaxation rate from $|\mathrm{Br}\rangle$ to $|\mathrm{Dx}\rangle$. Assuming a Boltzmann distribution of excitons between $|\mathrm{Br}\rangle$ and $|\mathrm{Dx}\rangle$ on the basis of a statistical ensemble of QDs,[16] the rate equation for the total number of the excitons N is given as $dN/dt=-n_{\mathrm{Br}}/\tau_{\mathrm{Br}}-n_{\mathrm{Dx}}/\tau_{\mathrm{Dx}}$, and thus, the decay rate in the TSM, $k_r(T)$, is given as

$$k_r(T) = \frac{\dfrac{1}{\tau_{\mathrm{Dx}}} + \dfrac{1}{\tau_{\mathrm{Br}}}e^{-\Delta E/k_{\mathrm{B}}T}}{1 + e^{-\Delta E/k_{\mathrm{B}}T}}. \quad (3)$$

The solid curve in Fig. 3(b) represents the calculated result for $k_r(T)$ using Eq. (3) with $\tau_{\mathrm{Br}}=8.4$ ns, $\tau_{\mathrm{Dx}}=110$ ns, and $\Delta E=6$ meV. The calculated result quantitatively explains

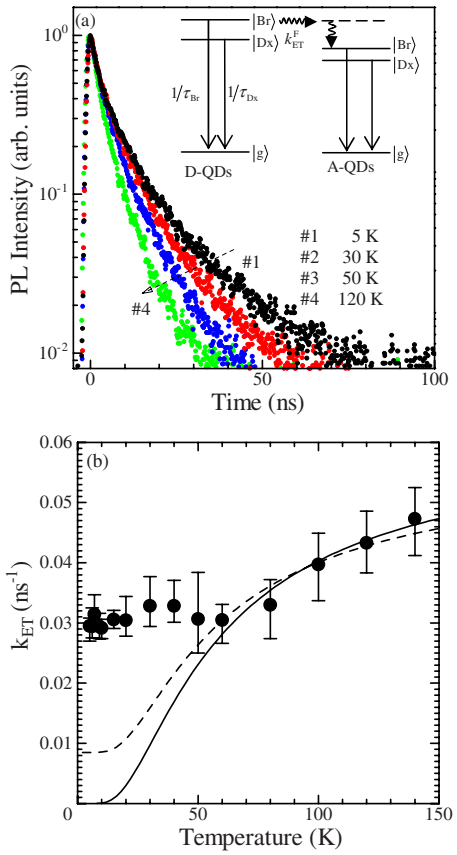

FIG. 4. (Color online) (a) PL-decay profiles of the D-QDs in the bilayer structure at 5, 30, 50, and 120 K. (b) Temperature dependence of the observed ET rate. Solid curve denotes the calculated result using Eq. (5) with $k_{ET}^{Br}=0.13$ ns^{-1}. Broken curve denotes the calculated result using Eq. (6) with $k_{ET}^{Br}=0.11$ ns^{-1} and $k_{ET}^{Dx}=0.008$ ns^{-1}.

the experimental one; namely, the decay rate becomes larger with an increase in temperature.

Next, we discuss the temperature dependence of ET dynamics. Figure 4(a) shows PL-decay profiles of the D-QDs in the bilayer structure at 5, 30, 50, and 120 K. The decay profiles at each temperature in the bilayer structure are faster than that in the monolayer structure of the D-QDs. These results obviously show the occurrence of the direct ET from the D-QDs to the A-QDs in the bilayer structure. The observed ET rate at the temperature of T, $k_{ET}^{obs}(T)$, can be estimated from the following expression: $k_{ET}^{obs}(T)=1/\langle\tau_{bilayer}(T)\rangle-1/\langle\tau_{monolayer}(T)\rangle$. Figure 4(b) shows the temperature dependence of $k_{ET}^{obs}(T)$. $k_{ET}^{obs}(T)$ exhibits clear temperature dependence and becomes larger as the temperature is increased.

Based on the Förster theory, the ET rate via dipole-dipole interaction is given by $k_{ET}^{Förster}=2\pi J^2\Theta/\hbar$, where Θ is the spectral overlap between a normalized donor PL and an acceptor absorption, and J is the dipole-dipole Coulomb coupling, estimated as $J^2=\mu_D^2\mu_A^2\kappa^2/R_{DA}^6n^4$. Here $\mu_D(\mu_A)$ is the donor (acceptor) transition dipole, κ^2 is an orientational average, n is the refractive index of the medium, and R_{DA} is the distance between donor and acceptor dipoles. In the present bilayer structure, it is considered that Θ does not depend on the temperature since the PL spectrum of the D-QDs and the absorption spectrum of the A-QDs are sufficiently overlapped. Furthermore, J does not include temperature-dependent parameters. Thus, $k_{ET}^{Förster}$ is expected to be independent of the temperature. However, as shown in Fig. 4(b), the experimental data of the ET rate obviously depends on the temperature.

We discuss the temperature dependence of $k_{ET}^{obs}(T)$ on the basis of the TSM. Since the bright-exciton (dark-exciton) state is optically active (passive), it is expected that the Förster ET process from $|Br\rangle$, which is based on a dipole-dipole interaction, is dominant. Considering the Förster ET rate from $|Br\rangle$ (k_{ET}^{Br}), the rate equation for the total number of the excitons should be modified as $dN/dt=-(1/\tau_{Br}+k_{ET}^{Br})n_{Br}-n_{Dx}/\tau_{Dx}$. Thus, the decay rate of the D-QDs in the bilayer structure, $k_r'(T)$, is given as

$$k_r'(T)=\frac{1/\tau_{Dx}+(1/\tau_{Br}+k_{ET}^{Br})e^{-\Delta E/k_BT}}{1+e^{-\Delta E/k_BT}}. \quad (4)$$

As a consequence, the ET rate on the basis of the TSM, $k_{ET}^{TMS}(T)$, is given from the relation of $k_{ET}^{TMS}(T)=k_r'(T)-k_r(T)$ as

$$k_{ET}^{TSM}(T)=\frac{k_{ET}^{Br}e^{-\Delta E/k_BT}}{1+e^{-\Delta E/k_BT}}. \quad (5)$$

The solid curve in Fig. 4(b) denotes a calculated result with use of the fitting parameter of $k_{ET}^{Br}=0.13$ ns^{-1}. For ΔE, we adopt the same value of 6 meV that used for the calculation of $k_r(T)$ shown in Fig. 3(b). The calculated result becomes larger with an increase in temperature. Although the Förster ET rate from $|Br\rangle$ (k_{ET}^{Br}) is independent in principle of the temperature, an increase in the thermal population on $|Br\rangle$ with an increase in temperature leads to the increase in $k_{ET}^{TMS}(T)$ as shown in Fig. 4(b). The calculated result quantitatively explains the temperature dependence of the observed ET rate (•) above 50 K. The thermal energy of k_BT for $T=60$ K is 5.2 meV that almost corresponds to the value of $\Delta E=6$ meV in the D-QDS. In the temperature region of $k_BT\geq\Delta E$, a quasithermal equilibrium between $|Br\rangle$ and $|Dx\rangle$ might be achieved by the adequate thermal energy even under the conditions in which the ET process from $|Br\rangle$ exists in the bilayer structure, which assures the appropriateness of Eq. (5).

On the other hand, there is a discrepancy between the calculated result and experimental one in the temperature region below 50 K and it becomes larger with a decrease in temperature. In the experiment, it is obvious that the ET is occurred even at 5 K from the comparison of the PL-decay profiles of the D-QDs in the monolayer and bilayer structures [Figs. 3(a) and 4(a)]. Contrary to the experiment, the calculated $k_{ET}^{TSM}(T)$ approaches zero at low temperature due to an increase in contribution of $|Dx\rangle$ to PL processes. In Eqs. (4) and (5), we assumed the ET rate from $|Dx\rangle$ to be zero. However, the lifetime of the dark exciton is long but finite. Thus, it is considered that the dipole-dipole interaction responsible for ET will not vanish. From the analysis of the temperature dependence of the PL-decay rate in the monolayer structure of the D-QDs, the life times of the bright and dark excitons

are obtained to be 8.4 and 110 ns, respectively. Based on the Förster model, the ET rate, $k_{\mathrm{ET}}^{\mathrm{Förster}}$, is inversely proportional to the lifetime of the donor dipole. Thus, the ET rate from $|\mathrm{Dx}\rangle$ is considered to be smaller than 1/10 of that from $|\mathrm{Br}\rangle$. By taking the ET rate from $|\mathrm{Dx}\rangle$ ($k_{\mathrm{ET}}^{\mathrm{Dx}}$) into consideration, the ET rate on the basis of TSM is modified as

$$k_{\mathrm{ET}}'^{\mathrm{TSM}}(T) = \frac{k_{\mathrm{ET}}^{\mathrm{Dx}} + k_{\mathrm{ET}}^{\mathrm{Br}} e^{-\Delta E/k_{\mathrm{B}}T}}{1 + e^{-\Delta E/k_{\mathrm{B}}T}}. \quad (6)$$

The broken curve in Fig. 4(b) represents a calculated result with use of $k_{\mathrm{ET}}^{\mathrm{Br}}=0.11\ \mathrm{ns}^{-1}$ and $k_{\mathrm{ET}}^{\mathrm{Dx}}=0.008\ \mathrm{ns}^{-1}$, where the ratio of $k_{\mathrm{ET}}^{\mathrm{Br}}$ and $k_{\mathrm{ET}}^{\mathrm{Dx}}$ was set to be equal to that of $1/\tau_{\mathrm{Br}}$ and $1/\tau_{\mathrm{Dx}}$. There is still discrepancy between the calculated result and experimental one in the temperature region below 50 K. The ET rate at 5 K is more than half of that at 140 K as shown in Fig. 4(b). Thus, the large value of the ET rate at low temperatures cannot be explained only by the contribution of the Förster ET from $|\mathrm{Dx}\rangle$.

The other typical ET process is the Dexter ET which originates from an electron-exchange mechanism. This is a short-range process since the Dexter ET requires an overlap of wave functions of the donor and acceptor. The mean distance between the D- and A-QDs in the bilayer structure is ~6 nm, which is much larger than the characteristic length of 0.1–0.5 nm for the Dexter ET. Furthermore, the ZnS shell in CdSe/ZnS QDs might prevent the electron exchange. Thus, the possibility of the Dexter ET from $|\mathrm{Dx}\rangle$ in the present bilayer structure can be ruled out.

One possible explanation of the deviation of the observed ET rate at low temperatures from the calculated result is as follows. The observed ET rate is almost constant in the temperature region lower than ~50 K. This phenomenologically suggests that the thermal population of $|\mathrm{Br}\rangle$ hardly depends on temperature; namely, the thermal equilibrium between $|\mathrm{Br}\rangle$ and $|\mathrm{Dx}\rangle$ is broken down. Note that the calculated result using Eq. (5) is based on the Boltzmann distribution between $|\mathrm{Br}\rangle$ and $|\mathrm{Dx}\rangle$. If the relaxation rate from $|\mathrm{Br}\rangle$ to $|\mathrm{Dx}\rangle$ is temperature dependent and decreases with a decrease in temperature, the thermal population of $|\mathrm{Br}\rangle$ is considerably enhanced in comparison with the case under the Boltzmann distribution. Tsitsishvili *et al.* theoretically suggest that the relaxation rate decreases with a decrease in temperature, taking account of phonon emission.[20] Thus, temperature dependence of the relaxation rate is a key factor for the observed ET rate in the low-temperature region. At present, a quantitative discussion is an open question.

IV. CONCLUSION

In summary, we have investigated the temperature dependence of ET between CdSe/ZnS QDs measuring photoluminescence dynamics in the bilayer structure consisting of differently sized QDs. Under the condition that the thermal energy is comparable to the splitting energy between the bright- and dark-exciton states and above, the observed ET rate is dominated by the thermal-population behavior of the bright-exciton state: The ET rate increases with temperature. In the lower temperature region, the observed ET rate is almost constant, which may be due to a breakdown of the thermal equilibrium between the bright- and dark-exciton states.

ACKNOWLEDGMENT

This work was supported in part by a Grant-in-Aid for Scientific Research from JSPS.

*tegi@a-phys.eng.osaka-cu.ac.jp

[1] U. Woggon, *Optical Properties of Semiconductor Quantum Dots* (Springer, New York, 1996).
[2] A. D. Yoffe, Adv. Phys. **50**, 1 (2001).
[3] Y. Masumoto and T. Takagahara, *Semiconductor Quantum Dots* (Springer, New York, 2002).
[4] V. I. Klimov, *Semiconductor and Metal Nanocrystals* (Marcel Dekker, Inc., New York, 2004).
[5] C. R. Kagan, C. B. Murray, and M. G. Bawendi, Phys. Rev. B **54**, 8633 (1996).
[6] S. A. Crooker, J. A. Hollingsworth, S. Tretiak, and V. I. Klimov, Phys. Rev. Lett. **89**, 186802 (2002).
[7] I. L. Medintz, H. T. Uyeda, E. R. Goldman, and H. Mattoussi, Nature Mater. **4**, 435 (2005), and references there in.
[8] E. Alphandéry, L. M. Walsh, Y. Rakovich, A. L. Bradley, J. F. Donegan, and N. Gaponik, Chem. Phys. Lett. **388**, 100 (2004).
[9] S. Dayal and C. Burda, J. Am. Chem. Soc. **129**, 7977 (2007).
[10] T. Franzl, T. A. Klar, S. Schietinger, A. L. Rogach, and J. Feldmann, Nano Lett. **4**, 1599 (2004).
[11] S. F. Wuister, R. Koole, C. M. Donegá, and A. Meijerink, J. Phys. Chem. B **109**, 5504 (2005).
[12] M. Nirmal, D. J. Norris, M. Kuno, M. G. Bawendi, A. L. Efros, and M. Rosen, Phys. Rev. Lett. **75**, 3728 (1995).
[13] A. L. Efros, M. Rosen, M. Kuno, M. Nirmal, D. J. Norris, and M. Bawendi, Phys. Rev. B **54**, 4843 (1996).
[14] S. Takeoka, M. Fujii, and S. Hayashi, Phys. Rev. B **62**, 16820 (2000).
[15] D. Kim, T. Mishima, K. Tomihira, and M. Nakayama, J. Phys. Chem. C **112**, 10668 (2008).
[16] S. A. Crooker, T. Barrick, J. A. Hollingsworth, and V. I. Klimov, Appl. Phys. Lett. **82**, 2793 (2003).
[17] C. de Mello Donegá, M. Bode, and A. Meijerink, Phys. Rev. B **74**, 085320 (2006).
[18] D. G. Kim, S. Okahara, M. Nakayama, and Y. G. Shim, Phys. Rev. B **78**, 153301 (2008).
[19] B. R. Fisher, H. J. Eisler, N. E. Stott, and M. G. Bawendi, J. Phys. Chem. B **108**, 143 (2004).
[20] E. Tsitsishvili, R. V. Baltz, and H. Kalt, Phys. Rev. B **67**, 205330 (2003).